Tutors

Dra. Maria Sarret Pons
Departament de Química Física
Universitat de Barcelona (UB)

Dr. Jordi Esquena Moret
Grup de Química de Superficies
Departament de Nanotecnologia Química i Biomolecular
Institut de Química Avançada de Catalunya (IQAC)
Consell Superior d'Investigacions Científiques (CSIC)

Grau de Química

Treball Final de Grau

Preparation and characterization of biomimetic materials, by synthesis and templating in structured liquids

Preparación y caracterización de materiales biomiméticos, mediante síntesis en líquidos estructurados, utilizados como plantillas

José Luis Capdevila Echeverria

June 2015

Universitat de Barcelona

Campus d'Excel·lència Internacional
B:KC Barcelona Knowledge Campus

"Do you know what the secret to success is?" I of course said no. He then said, "Just keep working."

Eric Kandel, quoted by (and said to) Eve Marder, interview in Current Biology 12:R5-R7 2007

First of all, I would like to acknowledge Institute of Advanced Chemistry of Catalonia (*Institut de Química Avançada de Catalunya, IQAC*) and Spanish National Research Council (*Consejo Superior de Investigaciones Científicas, CSIC*) for the *research introduction for university students (INTRO 2014) fellowship*. I would like to thank Dr. Jordi Esquena Moret having welcomed me in his research group for my Final Degree Project (*Treball Final de Grau, TFG*). It was a challenging and very profitable opportunity to study in his research group for the realization of the present project. I am deeply thankful to him, without his support, confidence and direction; this work would not be possible. I would also like to thank Dr. Maria Sarret Pons for her guidance, advice and discussion of the present work.

I am also grateful to the Final Degree Project committee for their time, care and consideration for the finalization of this project.

In addition, I would like to thank all members of the Colloid and Interfacial Chemistry Centre (formed by Dr. Jordi Esquena Moret and Dr. Conxita Solans Marsà groups) for their very useful help and support, particularly, Dr. Susana Vílchez Maldonado, Dr. Jonathan Miras Hernández, Dr. Jérémie Nestor, Dr. Tirso Emmanuel Flores Guia, Míriam Regué Griñó, Yoran Beldengrün, Montserrat Sindreu Grañe, and Laura Sobrevias Bonells.

Finally, a million thanks to my family and friends, their encouragement and love has gotten me through all the difficult times and I am grateful to them for all the chats and advice especially at the end when I was so busy.

Thank you all for everything!

REPORT

CONTENTS

1. SUMMARY

The following work has focused on the study, preparation and characterization of macroporous solid foams of hydroxyapatite, $Ca_{10}(PO_4)_6(OH)_2$, and collagen and gelatin hydrogels, of proteinaceous nature. The importance of these two types of materials, one inorganic and the other organic, lies in their possible combination to recreate both, features and functions, of bone tissue and, therefore, in their promising potential biomedical applications as a tissue replacement or regenerator. A major application could be its use for creating next generation prostheses which replace the current ones, usually made of stainless steel and/or titanium.

From the results obtained, it is confirmed the possibility of obtaining hydroxyapatite with high porosity and interconnectivity and low density using highly concentrated emulsions, following the sol-gel and EISA methodologies. In the protein hydrogels prepared by the addition of cross-linker before gelation method (mixing cross-linking method), a highly elastic gel was obtained. After freeze-drying, macroporous texture was observed. Thereby, such gels appear suitable for their combination with solid foams of hydroxyapatite, forming a bone-like composite or hybrid material.

Keywords: Hydroxyapatite, collagen, gelatin, emulsion, solid foam, hydrogel, biomimetic material, structured liquid.

2. RESUMEN

El siguiente trabajo se ha focalizado en el estudio, obtención y caracterización de espumas sólidas macroporosas de hidroxiapatita, $Ca_{10}(PO_4)_6(OH)_2$, y de hidrogeles de colágeno y gelatina, de naturaleza peptídica. La importancia de estos dos tipos de materiales, uno inorgánico y el otro orgánico, recae en su posible combinación para recrear, tanto en características y funciones, el tejido óseo y, por lo tanto, en sus prometedoras aplicaciones potenciales en biomedicina como sustituto o regenerador de dicho tejido. Una de las principales aplicaciones podría ser su utilización para la creación de prótesis de próxima generación que sustituyeran a las actuales, generalmente de acero inoxidable y/o titanio.

De los resultados obtenidos, se confirma la posibilidad de obtención de hidroxiapatita con elevada porosidad e interconectividad y de baja densidad mediante emulsiones altamente concentradas, siguiendo las metodologías sol-gel y EISA. En los hidrogeles de naturaleza proteica preparados mediante el método de adición de reticulante previa a la gelificación (método de mezclado-reticulación), se obtuvo un gel altamente elástico. Después de la liofilización, se observó una textura macroporosa. De este modo, este tipo de geles parecen adecuados para su combinación con espumas sólidas de hidroxiapatita, formando un material compuesto o híbrido parecido al hueso.

Palabras clave: Hidroxiapatita, colágeno, gelatina, emulsión, espuma sólida, hidrogel, material biomimético, líquido estructurado.

3. INTRODUCTION

3.1. BONE TISSUE

3.1.1. General description of bone tissue

Natural bone is a biomaterial having a complex structure [1], which currently can not be reproduced *in vitro* in the laboratory. Bones are authentic nanocomposites, consisting of hydroxyapatite nanocrystals imbibed in collagen-rich matrix. This structure is very complex and highly specialized to perform its different mechanical, metabolic and synthetic functions. Therefore, bone matrix is composed by two main phases in a nanometric scale: organic (65 wt.% of bone, mainly protein) and inorganic (35 wt.% of bone, mainly mineral), as it is described in Table 1 [2, 3].

Inorganic phase	Weight [%][(a)]	Organic phase
Hydroxyapatite	60	Collagen
Carbonate, water	4	–
Citrate	0.9	–
–	Variable	Non-collagenous proteins (osteocalcin, osteopontin, thrombospondin, sialoprotein, whey protein, etc.)
Sodium	0.7	–
Magnesium	0.5	–
Cl^-, F^-, K^+, Sr^{2+}, Pb^{2+}, Zn^{2+}, Cu^{2+}, Fe^{2+}	Variable	Polysaccharides, lipids, cytokines
–	Variable	Primary bone cells: osteoblasts, osteocytes, osteoclasts

[(a)] These compositions may vary slightly for different species and for different bones.

Table 1. Generic composition of bones *(table adapted from reference [3])*.

Bone mineral is mainly composed of hydroxyapatite, whereas collagen predominates in the protein part. Collagen acts as a support in which tiny crystal planes of hydroxyapatite join to

form bone. Bone collagen has a characteristic fibrous structure, whose diameter varies between 100 and 2000 nm. Similarly, the hydroxyapatite in the bone mineral is found in the form of nanocrystals, with size between 4x50x50 (nm).

The main role of minerals is to provide strength and rigidity to the bone, whereas collagen imparts resistance and flexibility. It is important to note that inorganic bone crystals are not directly linked to collagen, but connected through non-collagenous proteins, which represent between 3 and 5 wt.% of bone composition and provide active sites for biomineralisation and cell binding.

The amount of water present in bone is an important factor determining its mechanical behaviour. Lipids, around 2 wt.% of bone, are also required for cellular functions and they play a crucial role in biomineralisation. It is important to point out that biomineralisation degree is the most important factor to determine the mechanical capabilities of the bone.

When bone is initially deposited, it is structurally weak and disorganized. But after a few days the original bone becomes lamellar. In a macroestructural level, mature lamellar bone is distinguished in compact and spongy types. They differ in density, as their names indicate, and are organized in pores at multiple levels, from macro to nano, for the establishment of multiple functions, including the transport of nutrients, oxygen and body fluids.

The spongy or trabecular bone occupies about 20 % of total bone weight. It is lighter, has higher porosity and concentration of blood vessels than compact bone. The diameter of the pores can be from micrometres to millimetres. The compact or cortical bone is much denser and occupies about 80 % of total bone weight. It has lower porosity and concentration of blood vessels than spongy one. Pores have diameters of 10-20 μm and are separated by intervals of 200-300 μm [2].

There are five different types of cells associated with bone tissue: osteoprogenitor cells, osteoblasts, osteocytes, osteoclasts, and bone-lining cells. Nevertheless, the cells responsible for the formation of new bone are osteoblasts, which produce collagen and cover it with non-collagenous proteins which can retain minerals from blood flow, especially calcium and phosphate, creating new bone.

For proper growth and differentiation of osteoblasts, they must be found in a similar environment of the tissue being regenerated, achieving more favorable environments for their proliferation with nanometric porosities [2, 4, 5].

As it has been shown, hydroxyapatite and collagen are the two main components in bone tissue, and therefore, they will be described more in detail in the following sections.

3.1.2. Hydroxyapatite

Hydroxyapatite or hydroxylapatite belongs to the group of minerals known as apatite (apatite derived from the Greek απατείν (*apatein*) which means to deceive or mislead, as it is easily confused with other minerals like beryl or milarite). It differs from other apatites, since it contains water, as hydroxyl. Its molecular formula is $Ca_5(PO_4)_3(OH)$, sometimes denoted as $Ca_{10}(PO_4)_6(OH)_2$ to indicate that the crystal unit is formed by two entities. This is a type of calcium phosphate with a Ca/P molar ratio of 1.67. Its crystal system is hexagonal and its hardness is 5 on the Mohs scale. This mineral can have different colours: white, gray, yellow, green, violet, purple, red or brown. It is the kind of phosphate present in bones [5, 6, 7].

3.1.3. Collagen and gelatin

Collagen, from the Greek word for glue κόλλα (*kólla*), is the major insoluble fibrous protein in the extracellular matrix and in connective tissue. In fact, it is the single most abundant protein in the animal kingdom. There are at least 27 types of collagen, but 80-90 percent of the collagen in human body consists of types I, II, and III [8]. Type I is the most abundant in the organic phase of bone. Its main functions are structural and some remarkable properties are its high flexibility and tensile strength. It also has many desirable properties for cell growth. Being biocompatible, biodegradable, non-toxic, and with absence of antigenicity, collagen is very useful for bone tissue engineering and many other biomedical applications. It is also an osteoconductive and hemostatic agent (like hydroxyapatite). All collagen types have typical peptide sequences composed of periodically repeating groups of three amino acids. The first amino acid in each group is glycine, and the other two are proline (or hydroxyproline) and any amino acid (although these other two amino acids usually are, one, proline and, the other, hydroxyproline). The periodic frequency of proline conditions peculiar curl as a left-handed collagen helix (secondary structure known as α chain, with about three amino acid residues per turn). Glycine, without side chain, allows the approximation between different helices, so that three left-handed helices are twisted togheter into a right-handed triple helix or superhelix (tertiary structure known as procollagen or, after some chemical modifications, as tropocollagen). Next association steps will

give rise to fibrils and, finally, to fibres [5, 9]. Its different levels of structure are shown next, in Figure 1.

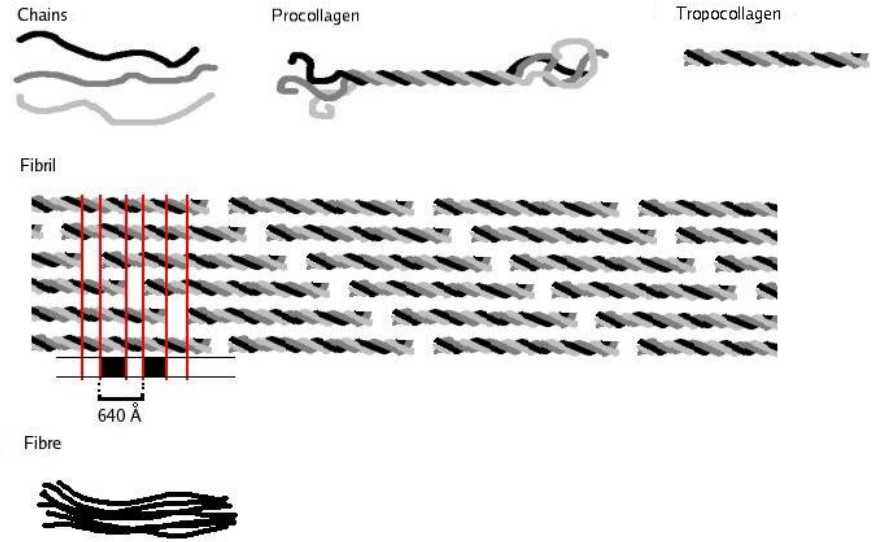

Figure 1. Three polypeptides coil to form tropocollagen. Many tropocollagens then bind together to form a fibril, and then many of these form a fibre *(Solitchka, 10/05/2015 via Wikimedia Commons, Creative Commons Attribution)*.

When collagen is denatured by boiling and allowed to cool, keeping it in an aqueous solution, it becomes a well-known substance, gelatin. It can also be obtained by physical and chemical degradation of collagen [10, 11].

3.2. EMULSIONS

Polymeric, organic or inorganic, foams exhibit specific properties such as high porosity and low density, which make them suitable candidates for hydroxyapatite recreation. Such materials can be obtained by using highly concentrated emulsions as templates, by polymerizing or cross-linking processes in the continuous phase of these emulsions.

3.2.1. Basic aspects of emulsions

Becher [12], in 1965, and Everett [13], in 1972, defined emulsions as thermodynamically unstable heterogeneous systems composed of at least two immiscible or partially miscible liquid phases, one of which is dispersed in the other in the form of droplets, with diameter generally greater than 0.1 μm.

Commonly added components to stabilize emulsions are surfactants. They are defined as amphiphilic molecules, characterized by having hydrophobic and hydrophilic sections. The main properties of surfactants are adsorption capacity in interfaces and the ability to form autoaggregates. These two properties (adsorption and self-assembly), are induced by intermolecular configurations that reduce unfavorable interactions [14]. Figure 2 shows schematically the two characteristic parts of a surfactant molecule.

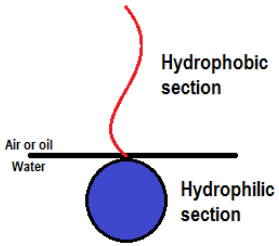

Figure 2. Schematic representation of a surfactant molecule.

The main classifications of the emulsions are based on two criteria: the nature of the phases and the volume fraction of dispersed phase (ϕ), as shown schematically in Figure 3. Emulsions can be generally classified as oil-in-water (O/W) when using hydrophilic or soluble surfactants in aqueous media and water-in-oil emulsions (W/O) when using lipophilic surfactants. Emulsions can also be classified according to the volume fraction of dispersed phase (ϕ), as diluted, concentrated and highly concentrated [15].

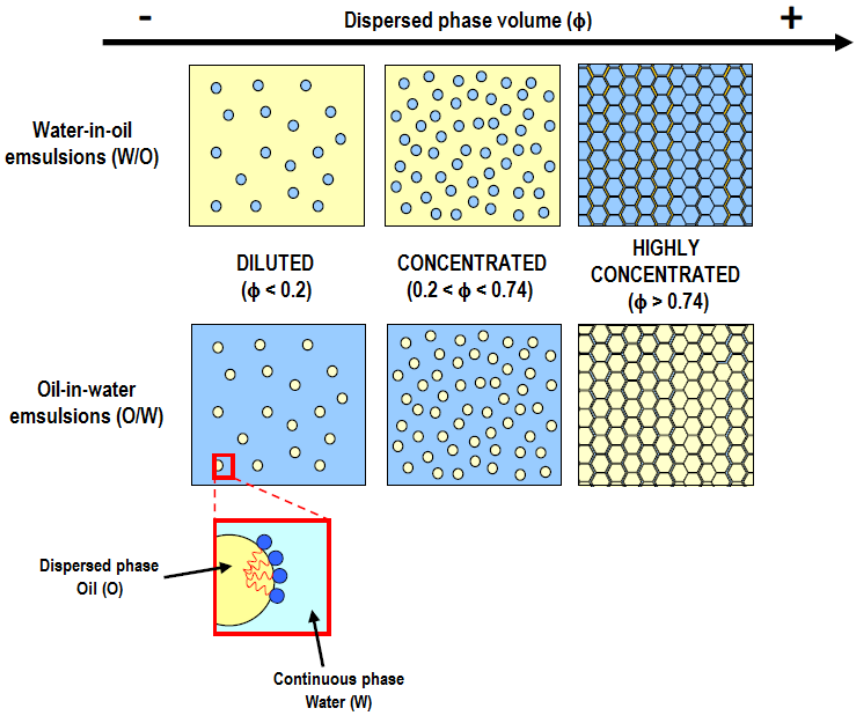

Figure 3. Classification of the emulsions according to the type of dispersed/continuous phase and depending on the volume fraction of dispersed phase (ϕ) *(figure reproduced from reference [15])*.

The emulsification involves the mixture of an oil phase, a water phase and a surfactant. During this process, the surfactant molecules are adsorbed at the liquid-liquid interface, producing a decrease in the interfacial tension. This decrease of the interfacial tension has two effects: favoring the emulsification and stabilizing emulsions. Overall, emulsification requires an input of energy. This energy is necessary because during the emulsification process the interfacial area is greatly increased, and consequently, an unfavourable positive Gibbs energy is induced, as shown by Equation 1:

$$\Delta_{form}G = \gamma\Delta A - T\Delta S \cong \gamma\Delta A > 0 \qquad \textbf{Equation 1}$$

Where $\Delta_{form}G$ is the variation of Gibbs energy in the emulsification process, ΔA is the new area generated by the emulsification, ΔS is the increase in entropy (positive since drops are produced), γ is the interfacial tension and T is the absolute temperature [15].

3.2.2. Highly concentrated emulsions as reaction media for the formation of porous materials

In recent decades, the use of highly concentrated emulsions as reaction media has generated a great interest. The high volume fractions of the dispersed phase allow to obtain materials with high porosity, and consequently, low density. A porous material can be obtained as a replica of the highly concentrated emulsion, after polymerizing and/or cross-linking in the emulsion continuous phase, and subsequently removing the dispersed phase. Thefore, the emulsion is the template that directs the formation of the porous material.

The earliest systematic studies on the formation of porous materials using highly concentrated emulsions were published by Bartl and von Bonin [16] and, later, by Barby and Haq [17]. The results demonstrated that a very wide variety of different porous materials could be obtained using such emulsions as reaction media. These systems are characterized by presenting high porosity with low densities (less than 0.1 g/cm^3).

One of the major classifications of porous materials is based on pore size. According to IUPAC accepted terminology [18], macroporous materials are those with pores above 50 nm, mesoporous materials have pores between 2 and 50 nm and microporous materials are those with pores smaller than 2 nm.

Macroporous solid foams, with very low density, can be obtained by one-step method [16, 17, 19]. This method consists in polymerizing or cross-linking into the continuous phase of the emulsion, followed by removal of the dispersed phase material and final drying to obtain porous foam (Figure 4).

In the case of sol-gel inorganic precursors, the formation of hydroxyapatite could be carried out in the external phase, following three steps [20, 21, 22]:

1) Formation of a sol, a colloidal dispersion of solid particles, into the continuous phase.
2) Gelation of the sol via sol-gel hydrolysis and condensation reactions.
3) Removal of solvent by evaporation.

This method, described by Vallet-Regí, was used to obtain macroporous hydroxyapatite [23, 54]. It involves the evaporation-induced self-assembly (EISA) methodology because the emulsion is formed after certain amount of solvent is evaporated [23, 24]. This general methodology will be used for the obtention of the porous hydroxyapatite in the present project.

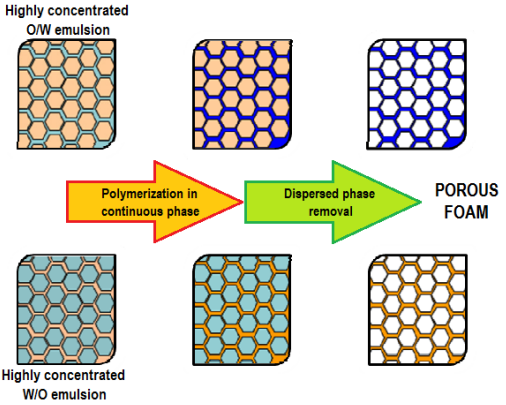

Figure 4. Schematic representation of the obtaining process of macroporous materials with hydrophobic or hydrophilic monomers/polymers, from W/O or O/W emulsions types, respectively *(figure reproduced from reference [15])*.

An interesting example of formation of macroporous hydroxyapatite, based on highly concentrated emulsions, is described as follows. A surfactant-in-alcohol emulsion (S/A emulsion) is formed. In such emulsions, the dispersed phase is the surfactant, which is insoluble in the alcohol phase (continuous phase), where the inorganic precursors were previously dissolved. First, a diluted emulsion is formed, but after alcohol (ethanol) is evaporated, the concentration of the dispersed phase increases and the emulsion becomes highly concentrated [23]. Therefore, surfactant concentration in the emulsion increases by removing alcohol, due to evaporation. Finally, macroporous hydroxyapatite is formed after calcination (Figure 5), which removes all the remaining organic components.

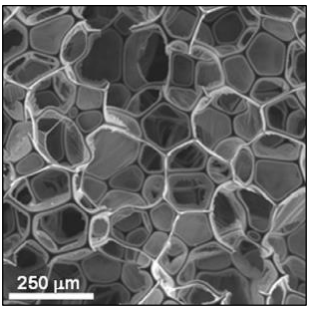

Figure 5. Example of macroporous hydroxyapatite, obtained in highly concentrated emulsions (surfactant-in-ethanol emulsions) as described in the literature *(figure reproduced from reference [25])*.

3.3. GELS

3.3.1. Basic aspects of gels

A gel is a non-fluid colloidal network or polymer network that shows viscoelastic flow behaviour. Many gels display thixotropy – they become fluid when agitated, but resolidify when resting. In general, gels are apparently solid, jelly-like materials. A gel can be formed by [26]: (i) a covalent polymer network, (ii) a polymer network formed through the physical aggregation of polymer chains, caused by hydrogen bonds, crystallization, helix formation, complexation, etc., (iii) a polymer network formed through glassy junction points, (iv) lamellar structures including mesophases, and (v) particulate disordered structures.

Gels can be classified in the following general types:

a) Aerogel: gel comprised of a microporous solid in which the dispersed phase is a gas [26].
b) Hydrogel: gel in which the swelling agent is water. The network component of a hydrogel is usually a polymer network. A hydrogel in which the network component is a colloidal network may be referred to as an aquagel [4, 26].
c) Organogel: gel in which the swelling agent consists predominantly of an organic solvent or a mixture of them [26].
d) Xerogel: a network formed by the removal of all swelling agents from a gel [26].

3.3.2. Protein polymer hydrogels

In the literature, it has been found that hydrogels are promising scaffold materials for cartilage tissue engineering, because of the high water retention and the ability to maintain the spherical morphology of encapsulated cells [27]. In special, collagen and gelatin hydrogels seem to be suitable options to recreate the soft organic matter of bone tissue, since collagen is the major protein component of this tissue. However, collagen has antigenicity, due to its animal origin. In contrast, gelatin seems a better choice, due to its much lower antigenicity, because it is a denaturalized protein. In addition, gelatin is much cost-effective than collagen. Nevertheless, the main limitation of gelatin for applications in tissue engineering is its high solubility in water. This limitation can be solved by cross-linking [10, 28, 29].

Various cross-linkers can be used to react with the free amino groups of the peptides constituting collagen or gelatin as glutaraldehyde, formaldehyde or ethylene glycol diglycidyl

ether [9, 27, 28]. However, these compounds have physiological toxicity. Therefore, in this study it has been used a naturally occurring cross-linking agent called genipin **1** (Figure 6), obtained from the fruits of *Gardenia jasminoides* Ellis, which has toxicity between 5000-10000 times less than glutaraldehyde [30, 31]. The use of this cross-linker is described in detail in the following section.

3.3.3. Cross-linking with genipin

Genipin **1** may react with the primary amino groups of lysine, hydroxylysine or arginine present in collagen and gelatin, forming new covalent bonds and cross-linking peptide chains, at ambient conditions and neutral pH. The proposed mechanism [32, 33] involves reacting the carboxymethyl group of the genipin **1** with the free amino group of lysine, hydroxylysine or arginine of collagen or gelatin to form a secondary amide and nucleophilic attack of other free amino groups (but of the same type involved) on an olefinic carbon of genipin **1**, producing an opening of the genipin **1** dihydropyran ring at an intermediate stage, leading to the formation of a tertiary amide. Several authors [32, 33] have also suggested that dimers and trimers of genipin **1** are formed during the cross-linking. This process is shown schematically in Figure 6, in which different bonds between chains of collagen or gelatin, represented as red lines, and the chemical structure of the cross-linking reaction between genipin **1** and collagen or gelatin are represented [15, 34, 35]. Dark blue colour is observed in the hydrogel, after cross-linking with genipin **1**.

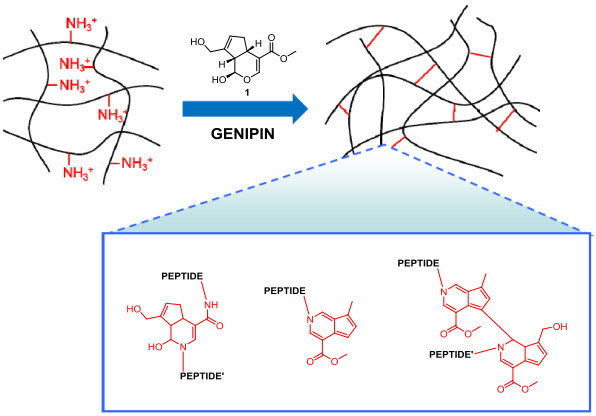

Figure 6. Schematic representation of cross-linking of collagen, or gelatin, with genipin **1** *(figure adapted from reference [15])*.

3.4. BIOMEDICAL APPLICATION: BIOMIMETIC POROUS COMPOSITES OF PROTEIN POLYMERS-REINFORCED HYDROXYAPATITE

The artificial joint prostheses have improved considerably since its introduction 40 years ago. The hip and knee prostheses are made of metal, usually stainless steel or titanium. Some implants have ceramic coatings, which are very smooth surfaces that reduce friction and wear in the joint. However, these prostheses cannot fully reproduce the properties and functions of bone tissues. The absence of bioadhesiveness and porosity in the prostheses prevents vascularisation and growth of osteoblasts. For these reasons, metallic prostheses have no autoregeneration capacity, and suffer mechanical wear over time.

This implies that such prostheses must be replaced frequently. An example is the femur head prostheses, which currently have a lifespan of about 15 years in young active patients. Hence, there is a great need for developing new biomechanical materials as bone substitutes [36]. In the literature, numerous methods have been described for obtaining macroporous hydroxyapatite [37, 38], although however, current mechanical and motor performance are inferior to metal prostheses and, for this reason, they continue being used as substitutes of bone.

In several studies, it has been found that vascularisation and osteoblast bioadhesion can be achieved by using synthetic macroporous materials made of hydroxyapatite [2, 39, 40]. Thus, there is a possibility that artificial prostheses based on hydroxyapatite could allow bone regeneration. Nonetheless, this has not still been achieved satisfactorily, and biomaterials produced *in vitro* have inferior biomechanical properties than natural bone. For that reason, stainless steel is the preferred available material. Regarding porous materials of hydroxyapatite described in the literature, their properties are far from reaching the features and functions of real bone tissue [41]. Synthetic porous materials of hydroxyapatite may be obtained by several methods, and templating in highly concentrated emulsions can be an interesting method, because the resulting porous structure has morphological similarities with natural bone.

Inorganic-organic porous composites, formed by a double interconnected matrix of hydroxyapatite and collagen or gelatin, could be a very interesting option (a hybrid material, with these components completely mixed, could also result another worthy way to investigate) [42] to solve the current drawbacks of titanium and stainless steel in prostheses. Similarly to natural bone, hydroxyapatite has high compressive strength, and the inclusion of collagen or gelatin

allows to increase fracture strength and toughness. Hence, it could be expected that porous composites of hydroxyapatite and collagen, or gelatin, possess better biomechanical capabilities than porous materials consisting solely of hydroxyapatite. For this reason, the present work will be focused on the study of porous hydroxyapatite and protein hydrogels.

4. OBJECTIVES

Given the importance of finding a suitable material, which biomimics bone tissue and can be applied in biomedicine to regenerate and replace natural bone, and taking into account the considerations explained in the introduction, the main objective of this work consisted in the study, obtention and characterization of macroporous hydroxyapatite and collagen and gelatin hydrogels.

The work plan is described below:

a) Selection of the most appropriate components: hydroxyapatite precursors, protein precursors (collagen and gelatin) and components of the emulsions (surfactant and continuous phase solvent).
b) Preparation and characterization of hydroxyapatite by infrared spectroscopy (IR), X-ray diffraction (XRD) and scanning electron microscopy (SEM).
c) Preparation of hydrogels of proteinaceous nature (collagen and gelatin) and study of their rheological properties, as function of the protein precursor, cross-linking agent, their concentrations, and temperature. As well as qualitative monitoring of the hydrogels formation and observation of their structure by scanning electron microscopy (SEM).
d) Feasibility study for obtaining macroporous hydroxyapatite, reinforced with collagen or gelatin.

5. EXPERIMENTAL SECTION

5.1. MATERIALS

5.1.1. Synthesis of macroporous hydroxyapatite foams

For the synthesis and cross-linking of hydroxyapatite, the following reagents have been selected:

a) Triethyl phosphite: **2**, $P(OCH_2CH_3)_3$, 98 wt.%, with a molecular weight of 166.16 g/mol. Supplied by Sigma-Aldrich. See molecule in Figure 7A, **2**.

b) Calcium nitrate tetrahydrate: $Ca(NO_3)_2 \cdot 4H_2O$, puriss. p.a., ACS reagent, 99-103 wt.%. It has a molecular weight of 236.15 g/mol. Supplied by Sigma-Aldrich.

c) Filtered deionized water: H_2O, Milli-Q® water (ultra-pure Millipore water system, Milli-Q_{plus} 185 filter). Supplied by Merck Millipore.

d) Pluronic® F 127: **3**, Poloxamer 407 (prill). It is a non-ionic surfactant (HLB = 18-23) consisting of a triblock structure composed of ethylene glycol and propylene glycol units, $HO(C_2H_4O)_{101}(C_3H_6O)_{56}(C_2H_4O)_{101}H$. It has an average molecular weight of 12600 Da (12600 g/mol). Supplied by BASF. See molecule in Figure 7B, **3**.

e) Ethanol: CH_3CH_2OH, absolute for analysis EMSURE® ACS, ISO, Reag. Ph Eur. Supplied by Merck Millipore.

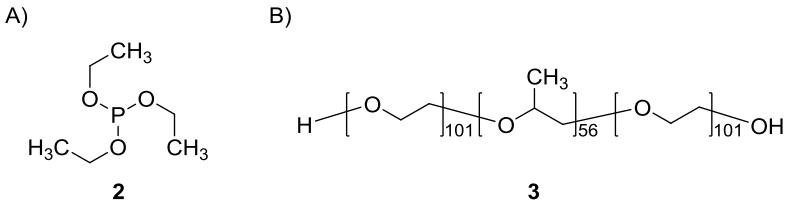

2 **3**

Figure 7. Formulas of A) triethyl phosphite **2** and B) Pluronic® F 127 **3**.

5.1.2. Preparation of protein hydrogels

For the preparation of collagen and gelatin hydrogels, the following reagents have been selected:

a) Peptan® P 2000 LD: porcine collagen peptides or hydrolyzed collagen with low density, with a content of type I collagen $\geq$ 90 wt.%. It has an average molecular weight of 2000 Da (2000 g/mol). Supplied by Rousselot.

b) Gelatin: from bovine skin, Type B (derived from lime-cured tissue). It is a heterogeneous mixture of water-soluble proteins of high average molecular weights, present in collagen (proteins are extracted by boiling skin, tendons, ligaments, bones, etc). It has an average molecular weight between 40000-50000 Da (40000-50000 g/mol) which correlates with a Bloom number (which is an indication of the strength of a gel formed from a solution of known concentration and this is directly proportional to molecular weight) between 175-225 (medium Bloom). Supplied by Sigma-Aldrich.

c) Genipin: **1**, 98 wt.%, with a molecular weight of 226.226 g/mol. It is a natural cross-linker for protein, collagen, gelatin and chitosan. Supplied by Challenge Bioproducts Co., Ltd. (Taiwan).

d) Phosphate buffered saline: PBS, in tablets. It provides a pH = 7.4 (physiological pH), at 25 ºC. It consists of a mixture of $Na_2HPO_4 \cdot 2H_2O$ (11.88 g/L) and KH_2PO_4 (9.08 g/L). Supplied by Sigma-Aldrich.

e) Glacial acetic acid: CH_3COOH, 100 wt.%, Ph Eur, BP, JP, USP, E 260. It has a molecular weight of 60.05 g/mol. Supplied by Merck Millipore.

f) Sodium hydroxide: NaOH, BioXtra, ≥ 98 wt.%, pellets (anhydrous). It has a molecular weight of 40.00 g/mol. Supplied by Sigma-Aldrich.

g) Filtered deionized water: H_2O, Milli-Q® water (ultra-pure Millipore water system, Milli-Q_{plus} 185 filter). Supplied by Merck Millipore.

5.2. APPARATUS AND INSTRUMENTAL

The equipment and instruments are listed below:

- Mettler Toledo AB204-S/FACT analytical balance with a precision of $\pm 10^{-4}$ g (maximum capacity: 220 g).
- Sartorius CPA3202-S top-loading balance with a precision of $\pm 10^{-2}$ g (maximum capacity: 3000 g).
- Heidolph MR Hei-Standard magnetic stirrer hot plate, with temperature controlled by means of Heidolph EKT3001 probe (maximum stirring capacity: 2500 rpm).
- IKA VORTEX 3 (vortex shaker).

- Vibromatric vibratory shaker, JP SELECTA, S.A.
- Memmert Waterbath WNB 7-45 (shaking bath with temperature control).
- Burdinola V21 Space ST 1500 fume hood.
- MBRAUN MB GB-2202-S glove box.
- Mettler Toledo Seven Easy pH-meter.
- HERAEUS T6 heating and drying oven (maximum temperature: 250 ºC).
- KOTTERMANN 2712 heating and drying oven (maximum temperature: 250 ºC).
- GHA 12/450 CARBOLITE horizontal tube furnace with compressed air flow (maximum temperature: 1200 ºC).
- Liebherr GX823 freezer (minimum temperature: -32 ºC).
- Christ Alpha 2-4 LD Plus lyophiliser, with pressure and temperature of ~0.03 mbar and -85 ºC, respectively.
- AR-G2 strain-controlled rheometer (TA Instruments).
- Hitachi TM-1000 Tabletop Microscope (Scanning Electron Microscopy, SEM).
- Nicolet Avatar 360 FT-IR spectrophotometer.
- Bruker D8 A25 Advance X-ray diffractometer with monochromatic Cu-Kα_1 and Cu-Kα_2 radiation (λ=1.5405 Å), primary parallel X-ray beam generated by a Göbbel mirror and the scattered beam analyzed by a lineal detector with 90-position sample loader.

5.3. METHODS AND PROCEDURES

5.3.1. Synthesis of macroporous hydroxyapatite foams

The 3D-macroporous HAp foams have been synthesized by the sol-gel technique [20, 21, 22, 37, 43] including a non-ionic surfactant, Pluronic® F 127 **3**, as macropore inducer in the accelerated evaporation-induced self-assembly (EISA) method.

Aqueous sols were prepared hydrolysing triethyl phosphite (TIP) **2** with Milli-Q® water for 24 h with magnetic stirring and adding it onto an ethanol mixture of non-ionic surfactant Pluronic® F 127 **3**. It is important to respect the hydrolysis reaction time to avoid uncompleted hydrolysed intermediates, i.e., diethyl phosphite or monoethyl phosphite, since this reduces further cross-linking (see Figure 8 for hydrolysis and polycondensation processes). Molar ratios of 0.06, 0.11, 0.44, and 11.0 of F127/TIP have been tested in order to obtain different degrees of

macroporosity. After 30 min continuous stirring, an aqueous 4 M calcium nitrate solution, $Ca(NO_3)_2 \cdot 4H_2O$, was added. The experimental added Ca/P molar ratio was varied between 1.67-1.85, since the minimum stoichiometric Ca/P molar ratio for the formation of HAp is 1.67 and increasing excesively this ratio could give rise to other types of calcium phosphates, instead of HAp [21, 22]. The mixed sol was stirred for 15 min and subsequently was aged at 60 ºC for 3-6 days, in order to enable further cross-linking. The resulting mixture was transferred into an open Petri dish and placed in an oven for 1.5 h at 100 ºC, to evaporate the solvent and to obtain the 3D-macroporous foams. Finally, in order to remove the surfactant and to obtain HAp, the sample was calcined at 550 ºC for 6 h in air atmosphere [23, 44, 45].

The resulting porous HAp foams were characterized by X-ray diffraction (XRD) in a Bruker D8 A25 Advance X-ray diffractometer using Cu-Kα radiation, determining qualitatively the crystalline phases using Diffracplus basic EVA, Diffracplus TOPAS and ICDD-PDF2 database software. Fourier transform infrared spectroscopy (FTIR) was performed in a Nicolet Avatar 360 FT-IR spectrophotometer. Scanning electron microscopy (SEM) was performed in a Hitachi TM-1000 Tabletop Microscope [23].

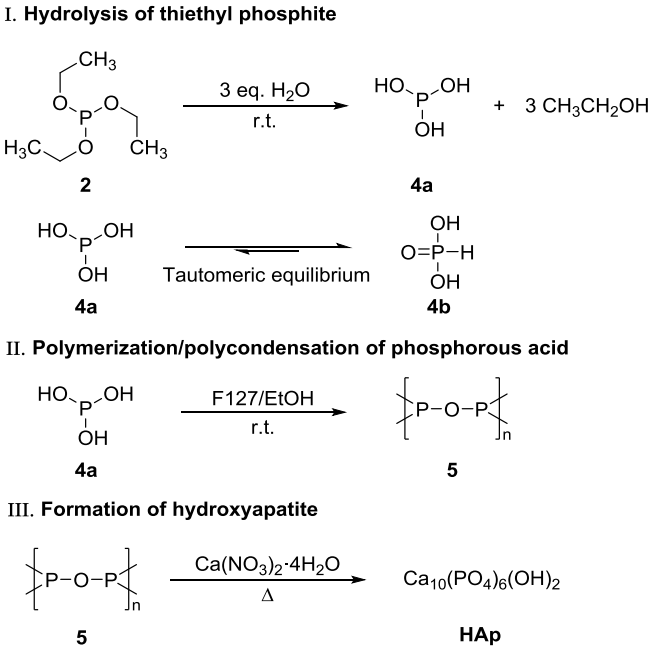

Figure 8. Global process involved in the formation of hydroxyapatite.

5.3.2. Preparation of collagen hydrogels

The hydrogels were prepared by two methods (Figure 9).

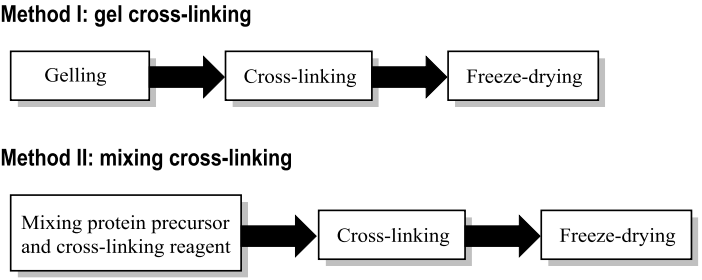

Figure 9. Schematic representation of the preparation methods of hydrogels used.

The details of these methods are described as followed.

5.3.2.1. Method I: Addition of cross-linker after gelation (gel cross-linking)

The 0.60 wt.% collagen solutions were prepared by dissolving Peptan® P 2000 LD (type I collagen) in 0.5 M CH_3COOH solution and vibrationally shaking at room temperature (~25 ºC) for 5 min. They were adjusted to neutral (pH = 7.4) by dropwise addition of 2 M NaOH solution, transferred to precut 60 mL syringes and incubated at 37 ºC in the oven for 1 to 24 h. Afterwards, 10 mL of PBS with genipin **1** were added (in control samples no genipin **1** content was added, only 10 mL of PBS were added), obtaining solutions with a total genipin **1** content of 0.30 wt.%. They were maintained at 37 ºC in the oven for 24 h.

Samples were frozen with dry ice and subsequently lyophilised for 24 h in order to inspect their microstructure by SEM in a Hitachi TM-1000 Tabletop Microscope (Figure 9, Method I) [9, 10, 27].

5.3.2.2. Method II: Addition of cross-linker before gelation (mixing cross-linking)

The collagen solutions were prepared by dissolving various wt.% Peptan® P 2000 LD (type I collagen) in PBS and vibrationally shaking at room temperature (~25 ºC) for 30 min. Then, certain wt.% contents of genipin **1** were added and the mixtures were uniformly mixed, first, in a shaking bath at 37 ºC for 10 min, and second, in a vibratory shaker at room temperature (~25 ºC) for 30 min. Afterwards, the mixtures were transferred to precut 60 mL syringes and allowed to stand for 2 days (Figure 9, Method II) [10].

5.3.3. Preparation of gelatin hydrogels

The gelatin stock solutions were prepared by dissolving gelatin (from bovine skin, type B, 175-225 Bloom) in PBS and magnetically stirring at 50 ºC for 24 h. The gelatin contents were 2, 6, and 10 wt.%. For these final gelatin concentrations, 4, 12, and 20 wt.% gelatin stock solutions were required, respectively. Genipin **1** stock solutions were prepared at different concentrations (1 and 0.25 wt.% in order to obtain final genipin **1** concentrations of 0.5 and 0.125 wt.%, respectively) by dissolving genipin **1** in phosphate buffer, at pH 7.4, by magnetically stirring for 1 h at room temperature (~25 ºC). The reaction of gelatin and genipin **1** occurred after mixing both solutions at a ratio of 1:1 (w/w) inside the precut 60 mL syringes [10, 11]. Mixed solutions were allowed to gel for 24 h at 25 ºC [28, 29, 30].

The rheological characterization was performed on freshly synthesized hydrogels using an AR-G2 strain-controlled rheometer (TA Instruments) at controlled temperature of 37 ºC. The geometry was plate-plate (standard steel parallel plates) of 40 mm diameter and the gap used was 2000 μm. Fresh samples were frozen at -32 ºC (Liebherr GX823 freezer) for 24 h and subsequently lyophilised (Christ Alpha 2-4 LD Plus lyophiliser) for 24 h (freeze-drying step) in order to observe their microstructure by means of a scanning electron microscopy (Hitachi TM-1000 Tabletop Microscope) (Figure 9, Method II) [28, 29, 35, 42].

5.3.4. Rheological study of hydrogels

The rheological study of the hydrogels was performed using dynamic oscillatory tests. In these tests, a sinusoidal stress (σ) with amplitude σ_0 is applied and a strain (γ) with amplitude γ_0 is measured simultaneously (Figure 10). Thus, a time shift (Δt) between the amplitudes of stress and strain, at a certain frequency (ω), occurs. The phase angle (δ) is calculated from the time shift (Δt) and frequency (ω), following the relationship shown in Equation 2.

$$\delta = \omega \Delta t \qquad \textbf{Equation 2}$$

The phase angle indicates the nature of the system: δ = 0º (elastic solid), δ = 90º (viscous liquid), and 0º < δ < 90º (viscoelastic system).

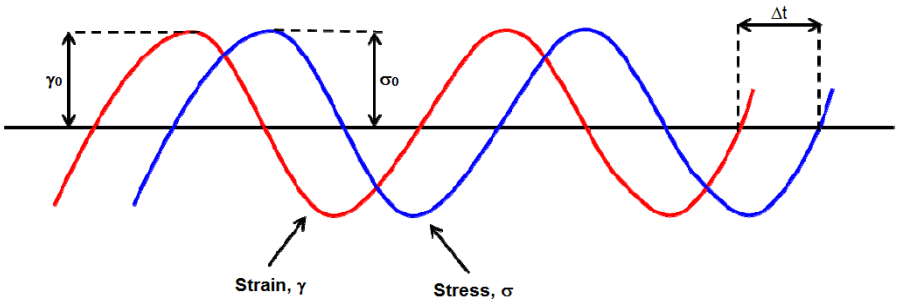

Figure 10. Sinusoidal curves for an applied oscillatory stress and its response in the form of a strain in a viscoelastic system *(figure reproduced from reference [15]).*

From γ_0, σ_0, and δ, the following rheological parameters are obtained: complex modulus, $|G^*|$ (it measures the resistance of the material to be deformed, see Equation 3), elastic or storage modulus, G' (it measures the elasticity of the material, which means the ability of the material to store energy, see Equation 4), and viscous or loss modulus, G'' (it represents the ability of the material to dissipate energy as heat, see Equation 5). The relation between elastic and viscous moduli is called δ tangent (it measures the energy dissipated in relation to the stored one, see Equation 6). This parameter indicates the viscoelastic behaviour of a material. The greater the elasticity, the smaller the δ tangent [30].

$$|G^*| = {}^{\sigma_0}/_{\gamma_0} \qquad \textbf{Equation 3}$$

$$G' = |G^*| \cos\delta \qquad \textbf{Equation 4}$$

$$G'' = |G^*| \sin\delta \qquad \textbf{Equation 5}$$

$$\tan\delta = {}^{G''}/_{G'} \qquad \textbf{Equation 6}$$

Such oscillatory tests can be divided into two categories: strain or frequency oscillatory tests. In the strain tests, the frequency (ω, rad/s or f, Hz being $\omega = 2\pi f$) and temperature are fixed and a strain sweep is performed whilst G' and G'' values are recorded. Generally, two distinct regions are detected based on the values of G' and G'' (Figure 11). The first region, known as linear viscoelastic region (LVR), is where G' remains virtually constant and independent of the applied strain. The second region is observed above a certain critical strain value, γ_{cr}, in which the G' and G'' values show a nonlinear behaviour and G' decreases with increasing strain. This critical value indicates the strain value where the structure of the material begins to be irreversibly fractured.

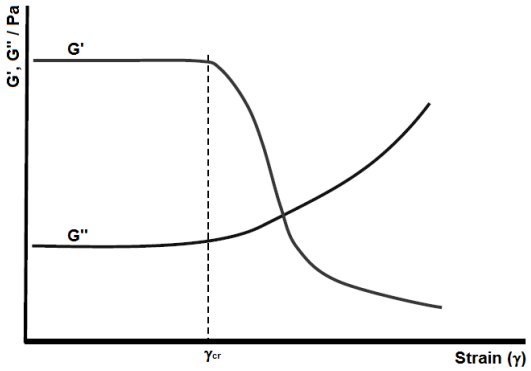

Figure 11. Representation of the response to a strain of a viscoelastic system, in an oscillatory test at a given frequency *(figure reproduced from reference [15]).*

From the critical strain (γ_{cr}) and the corresponding elastic modulus values, in the linear viscoelasticity region (G'_{LVR}), the cohesive energy density, E_c, can be calculated according to Equation 7 [46, 47, 48].

$$E_c = \frac{1}{2}\gamma_{cr}^2 G'_{LVR} \qquad \textbf{Equation 7}$$

The cohesive energy density value is a useful parameter for quantitatively evaluating the strength of the structure. If the energy applied is higher than the cohesive energy, then gel structure is greatly modified.

The viscoelastic behaviour of a system can also be studied by frequency oscillatory tests. In such tests, a strain within the linear viscoelastic region (a previous strain test is required) and the temperature are fixed. In this case, the *G'* and *G''* values are determined as a function of frequency (Figure 12).

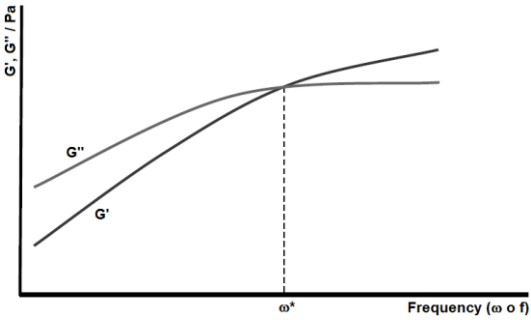

Figure 12. Representation of the response of a viscoelastic system in a frequency oscillatory test at a given strain *(figure reproduced from reference [15]).*

As shown in the diagram of Figure 12, two frequency regions are identified. At lower frequency values, the system is more viscous than elastic (*G''* > *G'*). However, in frequency values exceeding a critical frequency, ω^*, the system becomes predominantly elastic (*G''* < *G'*). The relaxation time is calculated as the inverse of ω^* [15, 49, 50, 51].

6. RESULTS AND DISCUSSION

6.1. SYNTHESIS OF MACROPOROUS HYDROXYAPATITE FOAMS

Following the procedure expressed in the previous section for the synthesis of macroporous hydroxyapatite foams, eight experiments have been performed. The amounts and molar ratios of reagents and precursors are indicated in the following tables (Tables 2-3).

Entry	Triethyl phosphite [μL]	Pluronic® F 127 [g]	Milli-Q® water [mL]	Ethanol [mL]	$Ca(NO_3)_2 \cdot 4H_2O$ 4 M [μL]
1	2.52	2.001	1.00	20.0	6.00
2	10.08	8.000	4.15	15.0	24.16
3	10.08	8.000	4.20	15.0	24.16
4	3.78	3.000	0.0016	80.0	10.00
5	20.16	16.000	0.0083	80.0	50.5
6	500	16.000	0.206	80.0	1250
7	2000	16.000	0.824	80.0	5000
8	4000	16.000	1.648	80.0	10000

Table 2. Amounts of reagents involved.

In Table 3, in addition to molar ratios, certain synthetic conditions are specified, as aging time, magnetic stirring speed during aging, and calcination temperature ramp. From Entries 1-5, it seemed that HAp was not obtained, proved by IR (Figure 13) and XRD (Figure 14) results, in addition to the fact that the final solid product was soluble in water, whereas HAp should be insoluble. However, macroporous pore size was obtained in all cases (Table 4). Important

considerations and procedimental changes (Table 3) were performed in order to achieve the formation of HAp, in Entries 6-8.

Entry	TIP/H_2O [mol/mol]	Ca/P [mol/mol]	F127/TIP [mol/mol]	Aging time [day]	Stirring speed during aging [rpm]	Calcination temperature ramp [ºC/min]
1	$2.59 \cdot 10^{-4}$	1.67	11.0	6	0	10
2	$2.50 \cdot 10^{-4}$	1.68	11.0	5	< 60	15
3	$2.47 \cdot 10^{-4}$	1.68	11.0	3	< 60	-
4	$2.43 \cdot 10^{-1}$	1.85	11.0	6	< 60	20
5	$2.50 \cdot 10^{-1}$	1.75	11.0	5	< 60	20
6	$2.50 \cdot 10^{-1}$	1.75	0.444	5	< 60	20
7	$2.50 \cdot 10^{-1}$	1.75	0.111	3	< 60	20
8	$2.50 \cdot 10^{-1}$	1.75	0.0555	4	< 60	2

Table 3. Molar ratios of reagents, aging times, magnetic stirring speeds during aging, and calcination temperature ramps.

These key changes were:

(i) Reducing water excess for TIP **2** hydrolysis, since high excesses seemed to hinder posterior cross-linking [20].

(ii) Increasing Ca concentration, since it was observed a deficience in Ca in the phosphate phase, as Monetite syn $CaPO_3(OH)$, Monetite $CaHPO_4$, and certain type of pyrophosphate were detected in the first experiments, instead of hydroxyapatite.

(iii) Decreasing F127/TIP molar ratio, which allowed to increase TIP **2** and Ca concentrations, and then obtaining higher amounts of product (Table 4).

(iv) Using low agitation speed during aging process, with a correct homogenisation during cross-linking.

(v) Reducing the temperature ramp during calcination at 2 ºC/min, allowing a larger and more robust HAp structure.

(vi) Finding suitable EtOH volume for the correct mixture with surfactant, from Entry 4 until Entry 8, a better homogenisation was observed (Table 2).

Among these changes, point (iii) was remarkably important and the results were the opposite as mentioned in certain literature [23], which recommended a F127/TIP molar ratio of 11 in order to obtain suitable macroporosity. As observed in Table 4, macroporous pore sizes were formed with a F127/TIP molar ratio less than 1. An aging time between 3-6 days was found to be suitable for cross-linking.

Complementing the information described in Table 4, different types of macroscopic and microscopic appearances of the products are illustrated in Table 5. Among experiments of Entries 6-8, which resulted in HAp formation, Entries 7 and 8 had more uniform pores, with shapes approximately circular, and also with good interconnectivities.

Entry	Product weight [mg]	Macroscopic appearance	Soluble in water?	Pore size (SEM) [nm][(a)]
1	4.6	Porous light brown powder	Yes	130-2400, macroporous[(b)]
2	27.7	Porous gray powder	Yes	200-4000, macroporous[(b)]
3	-	-	Yes (intermediate raw product)	-
4	10.1	Porous brown and gray particles	Yes	220-3800, macroporous[(c)]
5	41.8	Porous dark gray particles	Yes	400-5700, macroporous[(c)]
6	311.4	Porous dark gray structures	No	100-3600, macroporous[(d)]
7	1613.6	Porous gray-white structures	No	130-7100, macroporous[(e)]
8	3888.0	Porous gray-white structures	No	250-7100, macroporous[(e)]

(a) Pore size measured as pore diameter by scanning electron microscopy (SEM).
(b) Microscopic appearance: amorphous.
(c) Microscopic appearance: particulated.
(d) Microscopic appearance: cracked.
(e) Microscopic appearance: approximately circular.

Table 4. Weight, appearance, water solubility, and pore size (measured as pore diameter).

Among Entries 6-8, it seemed that lower F127/TIP molar ratio produced better macroporous HAp. Besides, the lowest calcination temperature ramp allowed to obtain the largest and the most robust HAp structures (Table 3). Lower temperature ramp seemed to produce weaker mechanical tensions between pores during calcination, in such a way that macrostructure was less affected and less fractured. Trace amounts of retained solvents, EtOH or H_2O, could also participate in the fracture of the structure when they were rapidly removed during calcination.

In Figure 13, it is observed that only IR spectra of Entries 6-8 correspond to HAp, when comparing to IR spectrum of the commercial HAp, Entry 1. Absorption bands located at 460 and 960 cm^{-1} are stretching modes of PO_4^{3-}, and the bands located at 560-600 and 1020 cm^{-1} correspond to bending modes of PO_4^{3-}. A characteristical OH^- stretch is observed at 3569 cm^{-1} in commercial HAp, but in synthetic HAp is not observed due to CO_3^{2-} substitution (CO_3^{2-} can also substitute PO_4^{3-}), which is difficult to eliminate at the calcination step. In this regard, it is observed a growth in carbonate bands (870, 1400-1450, and 1600-1650 cm^{-1}) in detrimental to hydroxyl or phosphate ones in the synthesized HAp. This kind of HAp is called as B-type HAp. In some spectra, some adsorbed water was detected, 2600-3600 cm^{-1} (absorption band becomes narrower under influence of thermal treatment) [52, 53, 54].

By means of XRD, the HAp identification was clearer than by IR for Entries 6-8, as it can be observed in Figure 14, if they are compared with the commercial HAp diffractogram. The other diffractograms were found not to be HAp, but other crystalline phosphate phases, as Monetite syn, $CaPO_3(OH)$; Monetite, $CaHPO_4$; and an unidentified pyrophosphate, which were soluble in water.

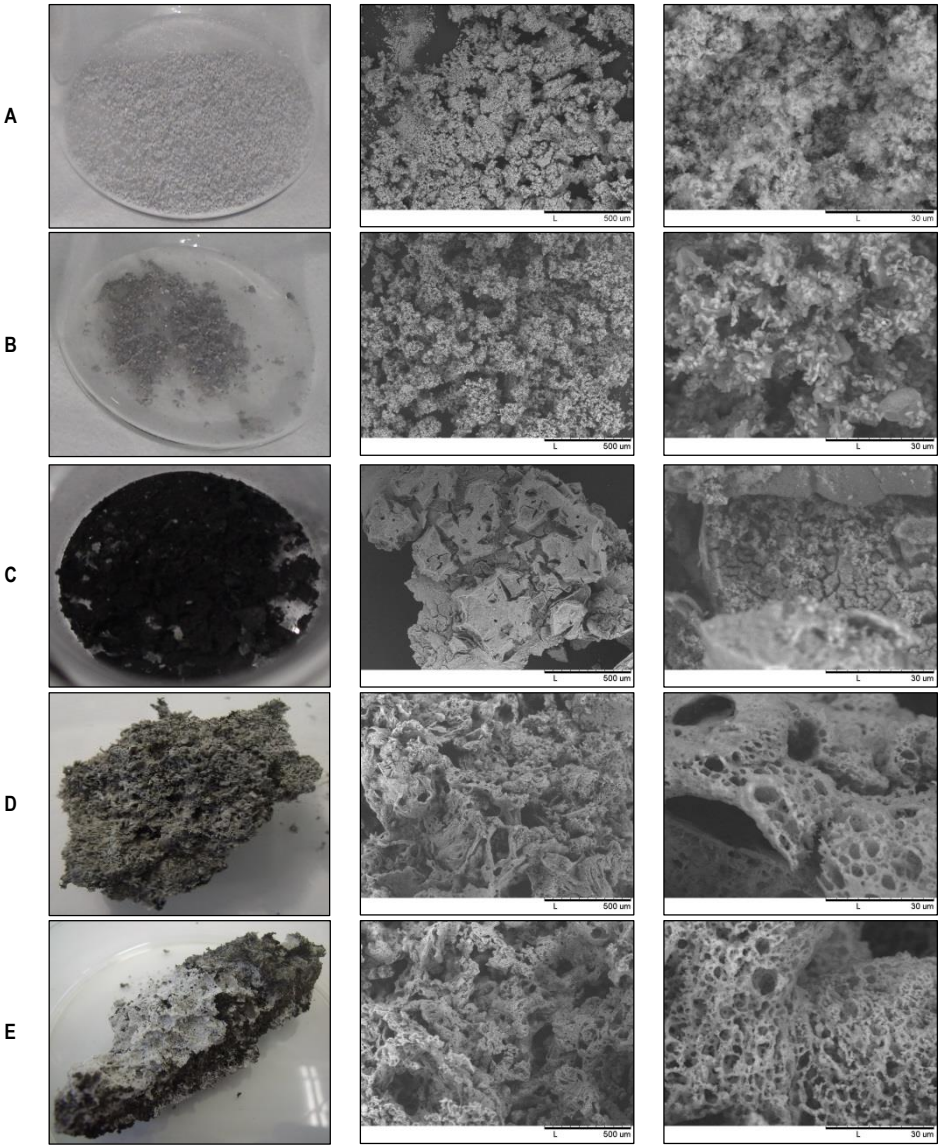

Table 5. Digital macrograph (first column of images), micrographs of x120 (second column of images), and micrographs of x2500 (third column of images) of the structures of: **(A)** Entry 2 (very similar to Entry 1), **(B)** Entry 5 (very similar to Entry 4), **(C)** Entry 6, **(D)** Entry 7, and **(E)** Entry 8. The different Entries make reference to the ones specified in Tables 2, 3, and 4.

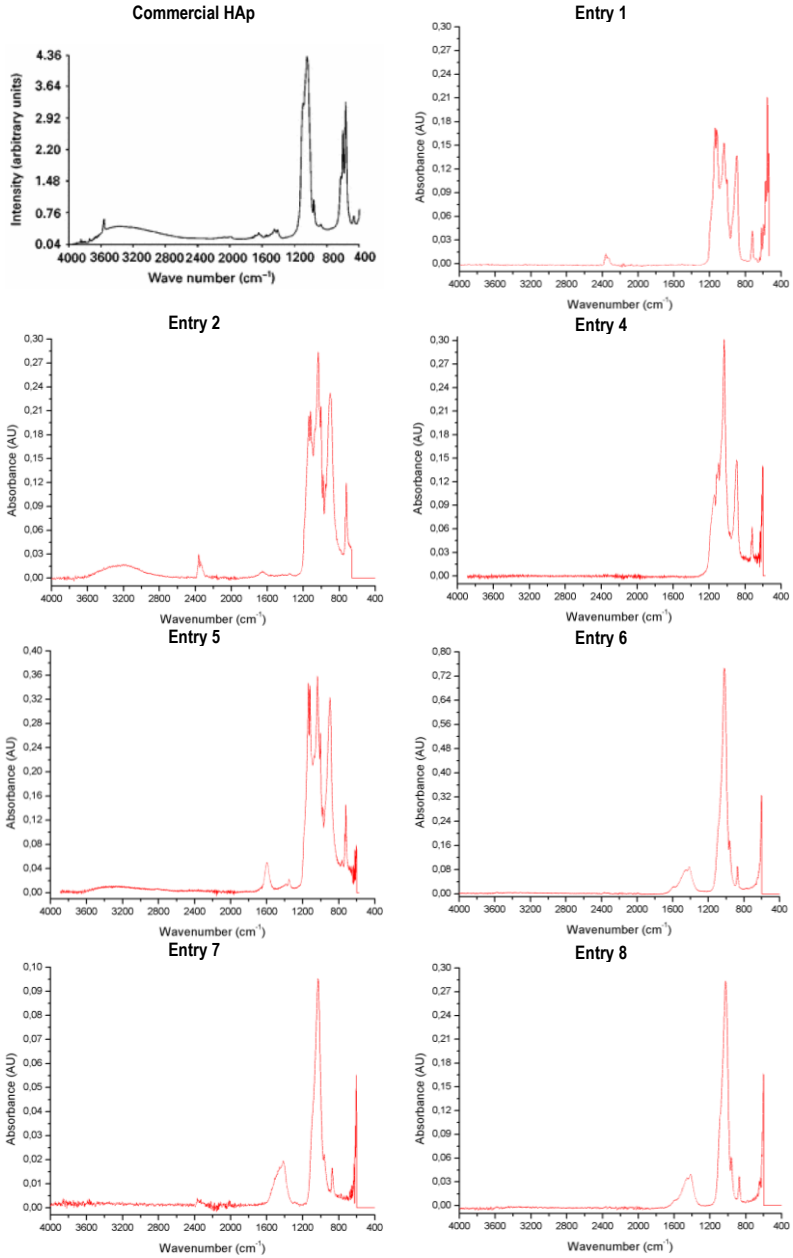

Figure 13. Product (Entries 1-8, except Entry 3) and commercial HAp (Merck, powder, for comparison) IR spectra *(commercial HAp IR spectrum is reproduced from [52])*.

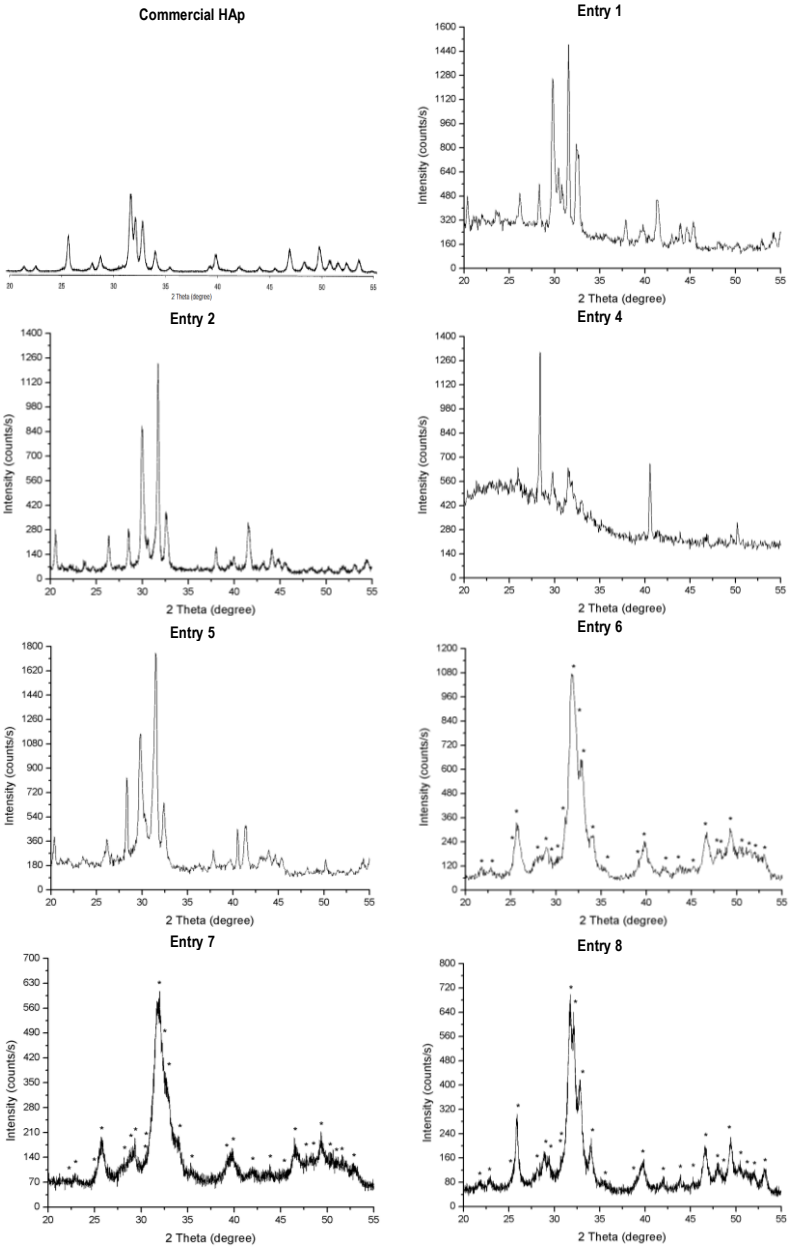

Figure 14. Product (Entries 1-8, except Entry 3) and commercial HAp (Fisher Scientific, USA, for comparison) XRD diffractograms *(commercial HAp XRD diffractogram is reproduced from [21])*.

6.2. PREPARATION OF PROTEIN HYDROGELS

6.2.1. Preparation of collagen hydrogels

6.2.1.1. Method I: Addition of cross-linker after gelation (gel cross-linking)

Dark blue and colourless collagenous liquid mixtures, with low viscosity, were obtained from this method, depending if samples contained genipin (GP) **1** or not (control samples), respectively. The same result was observed after 1 and 24 h (Figure 15). From this, it was inferred that no collagen hydrogel was formed, although cross-linking was observed for the dark blue evolution from colourless mixtures.

After lyophilisation, white and dark blue powders were observed for each case. SEM imaging showed flat non-porous material for control samples and flat and little porous (but not uniform) material for GP **1** samples (Tables 6-7).

Therefore, lack or little presence of porosity and no formation of hydrogels were observed in the first experiments. Thus, different collagen and GP **1** concentrations were studied, via Method II, which allows a more homogeneous mixing.

Entry	Time for gelling [h]	Macroscopic appearance	Microscopic appearance
1 (C)	1	White powder	Flat, non-porous
2	1	Dark blue powder	Flat, little porous (non-uniform pores)
3 (C)	24	White powder	Flat, non-porous
4	24	Dark blue powder	Flat, little porous (non-uniform pores)

Table 6. Description of time for gelling and macroscopic and microscopic appearances, after freeze-drying, of collagenous products. Entries 1 and 3 represent the control samples (C) for Entries 2 and 4, respectively.

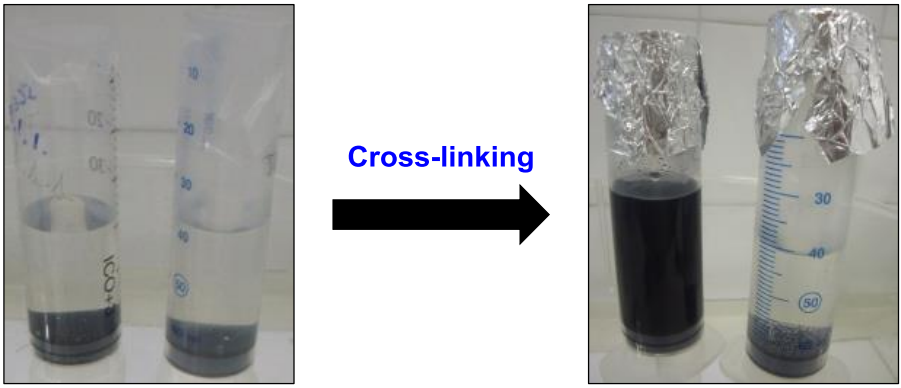

Figure 15. Representation of colour sample evolution, from colourless to dark blue, during cross-linking. Left image represents initial time of cross-linking process and right image represents final time of the process. Left syringes of each photo have GP **1** but not the right ones, the control samples (C).

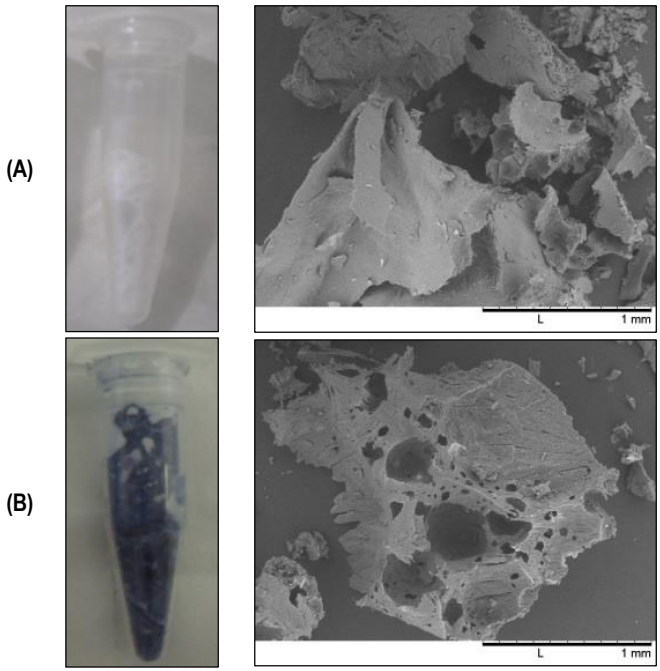

Table 7. Digital macrograph (first column of images) and micrographs of x80 (second column of images) of the structures of: **(A)** Entry 3 and **(B)** Entry 4. The Entries make reference to the ones specified in Table 6.

6.2.1.2. Method II: Addition of cross-linker before gelation (mixing cross-linking)

Firstly, Peptan® (collagen) concentration dependence was studied with GP **1** concentration fixed to 0.5 wt.% (Table 8). From this study, no hydrogel formation was observed. An increase in viscosity was observed with increasing Peptan® concentration, but gelation did not occur.

Entry	Peptan® [wt.%]	Genipin [wt.%]	Entry	Peptan® [wt.%]	Genipin [wt.%]
1 (C)	8	0	**10**	40	0.5
2	4	0.5	**11**	45	0.5
3	8	0.5	**12**	50	0.5
4	12	0.5	**13**	52	0.5
5	16	0.5	**14**	54	0.5
6	20	0.5	**15**	56	0.5
7	25	0.5	**16**	58	0.5
8	30	0.5	**17**	60	0.5
9	35	0.5	**18**	62	0.5

Table 8. Peptan® (not fixed) and GP **1** (fixed) concentrations tested in Method II with collagen. (C) means control sample, which did not contain GP **1**.

Secondly, GP **1** concentration dependence was studied with Peptan® (collagen) concentration fixed constant at 30 wt.%. This Peptan® concentration presented enough viscosity in the previous study and it was considered that higher cross-linker concentration would give rise to hydrogel formation (Table 9). However, hydrogel formation was unsuccessful again, despite an increase in viscosity induced by higher GP **1** concentration.

Entry	Peptan® [wt.%]	Genipin [wt.%]
1 (C)	30	0
2	30	3
3	30	6
4	30	9
5	30	12
6	30	15

Table 9. Peptan® (fixed) and GP **1** (not fixed) concentrations tested in Method II with collagen. (C) means control sample, which did not contain GP **1**.

In all results, up to this point, gelation was not observed, in spite of the cross-linking reaction, which was indicated by the appearance of dark blue colour. This absence of gelation was attributed to the low molecular weight of the collagen (2000 Da). It could be presumed that short collagen chains could not form the polymer network required for hydrogel formation.

Therefore, the next experiments were performed with gelatin with a much higher molecular weight (40000-50000 Da). It should be mentioned that gelatin and collagen are both similar proteins, but the gelatin tested posessed a much higher molecular weight than the available collagen.

6.2.2. Preparation of gelatin hydrogels

The formation of gelatin hydrogels was studied, and successful results were obtained. Table 10 shows the colour development and the gelling effect. After 24 h, hydrogels were observed in all cases, although little gelation was detected in Entry 1. From Table 10, it is important to remark that control hydrogel samples (Entries 1-3), which did not contain GP **1**, took longer to gel than samples with GP **1** (Entries 4-9). In absence of GP **1**, only intermolecular ionic forces and/or hydrogen bonding and Van der Waals interactions are present, in non cross-linked structures. However, cross-liking occurs in presence of GP **1**, and therefore covalent bonding between gelatin chains is produced, giving rise to a more elastic structure. Reference samples did not change the initial orange colour of gelatin, whereas cross-linked samples with GP **1** turned dark blue after 24 h, because of the reaction with GP **1** (Figure 16). Moreover, it was also observed that the higher the GP **1** concentration, the faster the gelation. This was related to higher cross-linking with higher GP **1** contents. In all cases, a quicker gelation was observed and more resistant hydrogels were formed with higher concentrations of gelatin; this seemed to be caused by an increase of intermolecular interactions between peptide chains.

Macroscopic aspect after 24 h can be observed in Figure 17. Control samples were orange and gelatin-GP samples were dark blue. Entry 1 was so little gelled that it was more like a liquid than a solid. This type of sample was used for the rheological study, which will be described at the end of this section.

Entry	Gelatin [wt.%]	Genipin [wt.%]	Reaction time [h][(a)]					
			0	0.5	1	2	3	24
1 (C)	2	0	light orange ungelled	light orange ungelled	light orange ungelled	light orange ungelled	light orange ungelled	light orange little gelled
2 (C)	6	0	orange ungelled	orange ungelled	orange ungelled	orange very little gelled	orange little gelled	orange fully gelled
3 (C)	10	0	dark orange ungelled	dark orange little gelled	dark orange gelled	dark orange gelled	dark orange fully gelled	dark orange fully gelled
4	2	0.125	light orange ungelled	light green-blue ungelled	green-blue ungelled	green-blue ungelled	dark green-blue very little gelled	dark blue fully gelled
5	6	0.125	orange ungelled	light green ungelled	green ungelled	green-blue very little gelled	dark green-blue little gelled	dark blue fully gelled
6	10	0.125	dark orange ungelled	light green ungelled	green-blue very little gelled	dark green-blue little gelled	dark green-blue gelled	dark blue fully gelled
7	2	0.5	light orange ungelled	light green ungelled	green-blue ungelled	dark green-blue very little gelled	dark green-blue little gelled	dark blue fully gelled
8	6	0.5	orange ungelled	green little gelled	dark green-blue gelled	dark green-blue fully gelled	dark green-blue fully gelled	dark blue fully gelled
9	10	0.5	dark orange ungelled	dark green gelled	dark green fully gelled	dark green fully gelled	dark green-blue fully gelled	dark blue fully gelled

(a) For Entries 1-3 (control samples, (C)), reaction time is understood as only elapsed time because there is no cross-linking reaction, in these cases the gelation observed is caused only by intermolecular forces as ionic forces, hydrogen bonding, and Van der Waals interactions.

Table 10. Colour development and gelling effect of the gelatin-GP mixtures and control samples (C) at different gelatin and GP **1** concentrations as a function of reaction time.

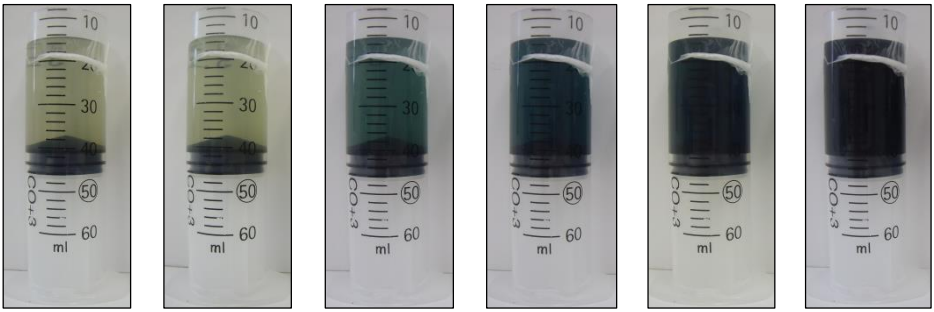

Figure 16. Example of colour evolution, from light orange to dark blue, during the cross-linking process of Entry 4 in Table 10.

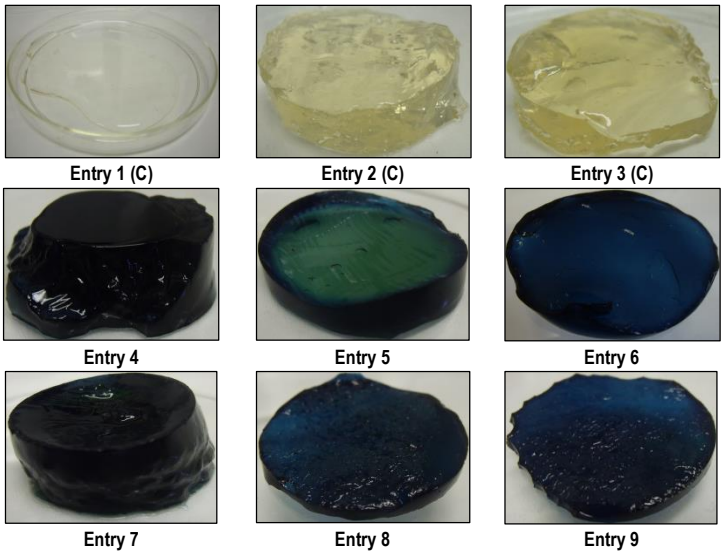

Figure 17. Macroscopic appearances of hydrogels formed of Entries 1-9 in Table 10 after 24 h. In Entry 1 (C), the consistency of the hydrogel was more like a liquid than a solid.

Microscopic observations by SEM of freeze-dried hydrogels showed a three-dimensional interconnected porous structure in all cases (Figure 18). It can be observed an increase in pore size when gelatin concentration was increased, and also when increasing the GP **1** content. Interconnection also seems to increase in gelatin-GP samples, respect to the control samples.

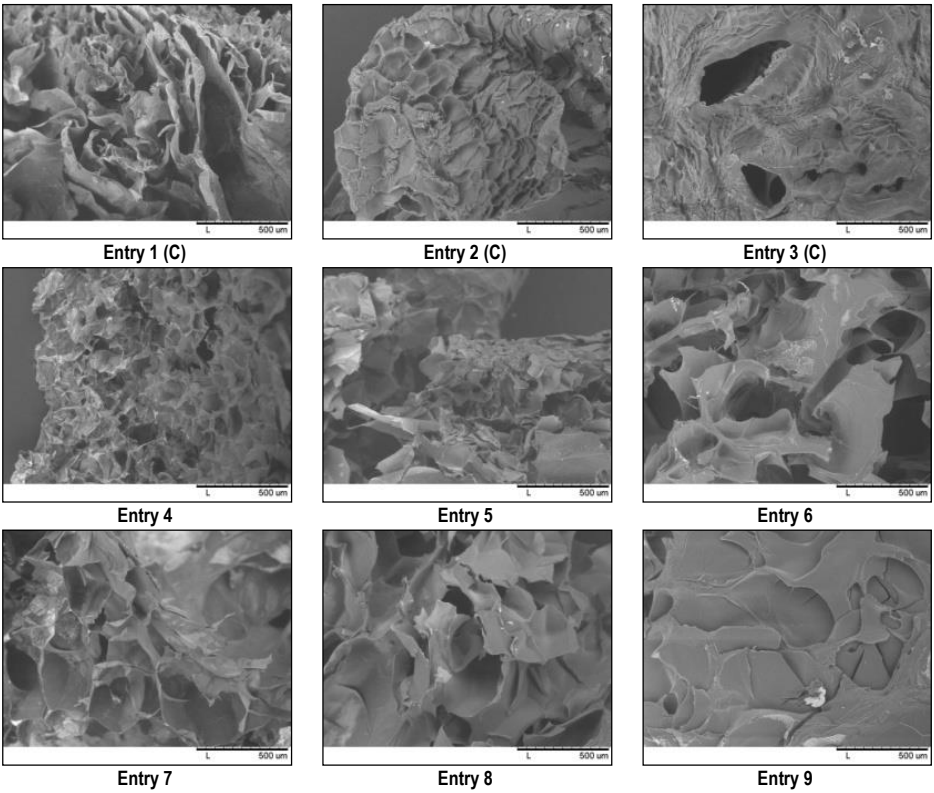

Figure 18. Microsgraphs (x120) of hydrogels formed in Entries 1-9 of Table 10, taken after freeze-drying.

A rheological study of the hydrogels obtained was carried out in order to determine their viscoelastic behaviour. A strain sweep test was performed at 37 ºC and 1 Hz to evaluate the storage (*G'*) and loss (*G''*) moduli of gelatin hydrogels.

In Table 11, a high increase in *G'* and *G''* values (measured at 1 % of strain, in the LVR) was observed when increasing GP **1** concentration, but a lower increase was observed when increasing gelatin concentration (when fixing the GP **1** content), except for Entries 5 and 6 where *G'* and *G''* are quite similar. It can also be observed that the storage modulus was higher than the loss modulus in all cases. From these results, a more elastic than viscous behaviour was inferred, and thereby, a material more solid than liquid was obtained in Entries 5-9. Moreover, it was observed that the solid behaviour increased when GP **1** and gelatin concentrations were increased. This change was more obvious with the variation of the GP **1** content. This rheological response is attributted to the higher density of cross-links. The

presence of cross-links reduces the intrinsic mobility of the polymer chains, and then increases the relaxation times. Consequently, at short times the materials show an elastic behaviour. In Figure 19, the results of strain sweep tests are shown.

Entry	Gelatin [wt.%]	Genipin [wt.%]	G' [Pa]	G'' [Pa]	E_c [J·m^{-3}]
1 (C)	2	0	-	-	-
2 (C)	6	0	-	-	-
3 (C)	10	0	-	-	-
4	2	0.125	-	-	-
5	6	0.125	76	0.7	0.03
6	10	0.125	66	0.9	0.1
7	2	0.5	884	19.6	0.7
8	6	0.5	962	19.9	2.9
9	10	0.5	1461	29.7	5.5

Table 11. *G'*, *G''* and E_c values of Entries 1-9. In Entries 1-4, measures were not possible due to transition from solid to liquid states at the experimental temperature, 37 ºC. *G'* and *G''* values are taken at 1 % strain, in the LVR.

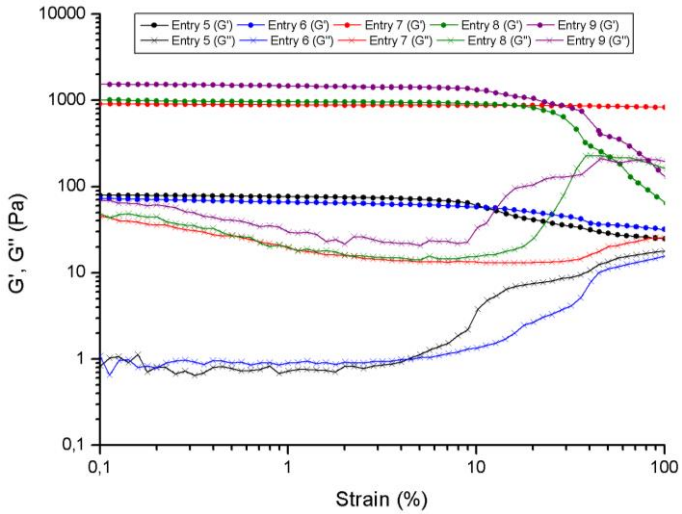

Figure 19. Strain sweep representation for the Entries 5-9 in Table 11 in an oscillatory test at a frequency of 1 Hz.

For Entries 1-4, rheological determinations could not be performed due to the transition from solid to liquid at the controlled temperature, 37 ºC. From Figure 19, the cohesive energy (E_c) values were determined for Entries 5-9 (Table 11). This parameter also increased more when increasing GP **1** concentration than when gelatin content increased. This means that cross-linking, by covalent bond formation, is the main structural parameter that determines the gelation of the gelatin-GP hydrogels.

A frequency sweep test was also performed at 37 ºC and 1 % strain to characterize the viscoelastic behaviour of the samples. In Figure 20, it can be observed that *G' > G''* at frequency values less than ω^*, which means that the hydrogels obtained were more elastic than viscous in the frequency region studied.

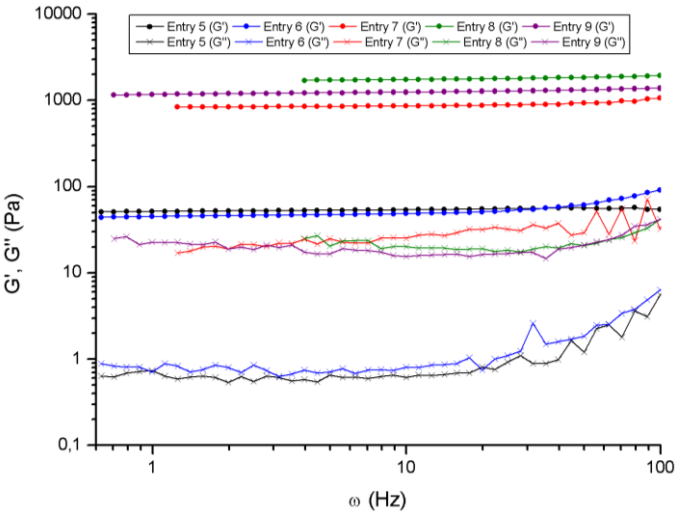

Figure 20. Frequency sweep representation for the Entries 5-9 in Table 11 in an oscillatory test at a strain of 1 %.

6.3. FEASIBILITY STUDY FOR OBTAINING MACROPOROUS HYDROXYAPATITE REINFORCED WITH COLLAGEN OR GELATIN

The results obtained in this research allow to formulate the hypothesis that artificial bone tissue could be simulated *in vitro*, by obtaining macroporous hydroxyapatite and reinforcing it with imbibed cross-linking gelatin hydrogels.

A novel hydroxyapatite/gelatin reinforced porous material could be obtained, by imbibing macroporous hydroxyapatite with gelatin, previous to its gelation. This seems also possible for collagen if done with a higher average molecular weight, since, then, gelation seems that could occur, as with gelatin.

The formation of these novel biomaterials could be studied in the future. This subject could be a very interesting and promising continuation of the present work.

7. CONCLUSIONS

The interpretation of the results has allowed to reach the following conclusions:

I. Synthesis of macroporous hydroxyapatite foams

a) Macroporous hydroxyapatite has been synthesized, by a method based on previous publications [23, 25, 37, 45]. The synthesis has been optimized, by studying the influence of the different parameters.

b) Water concentration in stoichiometric excess was required for TIP **2** hydrolysis. Ca concentration, in excess respect to the stoichiometric molar ratio of Ca/P = 1.67, was also required to obtain hydroxyapatite.

c) The volume of ethanol, used as solvent, was optimized in order to obtain a good homogeneity during the whole process.

d) Low agitation speed, < 60 rpm, was enough for good homogenisation during the sol-gel reactions, and an aging time between 3-6 days was suitable for cross-linking.

e) Hydroxyapatite was identified by XRD and IR spectra, and also by its water insolubility. The results confirmed the synthesis of hydroxyapatite.

f) A F127/TIP molar ratio smaller than 1 was suitable for the formation of a macroporous structure.

g) Slow temperature ramps during calcination, 2 ºC/min, leaded to less fractured macroporous hydroxyapatite.

II. Preparation of collagen hydrogels

a) Formation of collagen hydrogels was not observed after the addition of genipin **1**.

b) An increase in viscosity was observed when increasing both collagen and genipin **1** concentrations. However, elastic gels were not observed by rheology, even at very high concentrations of both collagen and genipin **1**. Consequently, it was concluded that gelation had not occurred.

c) The absence of gelation was attributed to low average molecular weight of the collagen molecule (2000 Da). The chains could be too short for producing a polymer network that would increase the elastic modulus (*G'*).

III. Preparation of gelatin hydrogels

a) Gelatin hydrogels were obtained by adding genipin **1**. The rheological determinations showed that the elastic modulus (*G'*) was much higher than the viscous modulus (*G''*), which is typical of hydrogels. The formation of gelatin/genipin hydrogels was achieved thanks to the high molecular weight of gelatin, which is much higher than the molecular weight of the collagen, previously used.

b) Control samples, in absence of genipin **1**, remained orange whereas gelatin/genipin samples became dark blue. This change was attributed to cross-linking reactions.

c) Samples in presence of genipin **1** gelled much faster than samples in absence of genipin **1**, demonstrating the formation of cross-links between gelatin chains.

d) Gelation velocity increased with genipin **1** concentration. This was attributed to a higher degree of cross-linking. Moreover, the elastic modulus (*G'*) also increased with genipin **1** concentration. These results clearly confirmed the formation of gelatin-genipin-gelatin covalent bridges, demonstrating cross-linkage.

e) The increase in gelatin concentration also increased both gelation velocity and gel elastic modulus (*G'*).

f) The cohesive energy (E_c), calculated from the rheological properties, greatly increased with the increase in genipin **1**, but increased slightly with gelatin content. This is consistent to a gelatin polymer network, which is cross-linked with genipin **1**.

A method for the synthesis of macroporus hydroxyapatite has been optimized. The macropores are formed by the templating effect of surfactant droplets dispersed in the ethanol/precursors mixture, as described in a previous publication [23]. The method allows formation of large porous monoliths, and it could be scaled-up to obtain large porous blocks, resembling natural bone. The formation of cross-linked gelatin materials has also been achieved. Therefore, the synthesis of porous hydroxyapatite/cross-linked gelatin composite materials can be possible. This material, consisting of hydroxyapatite reinforced with gelatin, could be more similar to natural bone, and thus, it could be considered a biomimetic material. The hydroxyapatite/gelatin composite could simulate the features and functions of bone tissue. Therefore, the synthesis of hydroxyapatite/gelatin composites can be a very interesting subject for research, and possible studies as bone substitute could be carried out. This subject can be the scope of a future research.

8. REFERENCES

1. Steele, D. G.; Bramblett, C. A. The Anatomy and Biology of the Human Skeleton, Revised ed.; Texas A&M Univ. Pr.: Austin, 1988.
2. Fundación MAPFRE. Martínez, E. B.; Muñoz, F. L.; Pellejero, A. L.; Gil, A. T.; Gordo, M. C.; Escobar, M. M. Bone composition study for an appropriate regeneration with implanted materials http://www.mapfre.com/fundacion/html/revistas/patologia/v4n3/pag02_01_res.html (accessed Apr 19, 2015).
3. Murugan, R.; Ramakrishna S. Development of nanocomposites for bone grafting. *Compos. Sci. Technol.* **2005**, *65*, 2385-2406.
4. Escuela de Medicina. Pontificia Universidad Católica de Chile. Tejido conectivo http://escuela.med.puc.cl/publ/Histologia/paginas/co26277.html# (accessed Apr 19, 2015).
5. II Congreso Virtual Hispanoamericano de Anatomía Patológica. Serrano, S. Estructura y función del hueso normal http://www.conganat.org/iicongreso/conf/018/matriz.htm (accessed Apr 19, 2015).
6. Rangel, N. A.; de Alva, H. E.; Romero, J.; Rivera, J. L.; Álvarez, A.; García, E. Síntesis y caracterización de materiales reforzados ("composites") de poliuretano poroso/hidroxiapatita. *Rev. Iberoam. Polim.* **2007**, *8*, 2, 99-111.
7. Mineralogical database. Hydroxylapatite http://www.mindat.org/min-1992.html (accessed May 9, 2015).
8. Lodish, H.; Berk, A.; Zipursky, S. L.; Matsudaira, P.; Baltimore, D.; Darnell, J. *Molecular Cell Biology*, 4th ed.; W. H. Freeman: New York, 2000.
9. Zhang, X.; Chen, X.; Yang, T.; Zhang, N.; Dong, L.; Ma, S.; Liu, X.; Zhou, M.; Li, B. The effects of different crossing-linking conditions of genipin on type I collagen scaffolds: an in vitro evaluation. *Cell Tissue Bank* **2014**, *15*, 531-541.
10. Lien, S.; Li, W.; Huang, T. Genipin-crosslinked gelatin scaffolds for articular cartilage tissue engineering with a novel crosslinking method. *Mater. Sci. Eng., C* **2008**, *28*, 36-43.
11. Zandi, M. (2008). *Studies on the Gelation of Gelatin Solutions and on the Use of Resulting Gels for Medical Scaffols*. Ph. D. Thesis. University of Duisburg-Essen. Germany.
12. Becher, P. *Emulsions: Theory and practice*, 2nd ed.; Reinhold Publishing Corp.: New York, 1965.
13. Everett, D. H. Definitions, Terminology and Symbols in Colloid and Surface Chemistry. *Pure Appl. Chem.* **1972**, *31*, 579-638.
14. Rosen, M. J.; Kunjappu, J. T. *Characteristic Features of Surfactants (Chapter 1), in: Surfactants and Interfacial Phenomena*, 4th ed.; John Wiley & Sons, Inc.: USA, 1978.
15. Miras, J. (2015). *Formación y propiedades de espumas macroporosas de quitosano obtenidas a partir de emulsions altamente concentradas*. Ph. D. Thesis. University of Barcelona. Spain.
16. Bartl, V. H.; Prof, H.; Ing, E. Uber die polymerisation in umgekehrter emulsion. *Macromol. Chem. Phys.* **1962**, *57*, 74-95.
17. Barby, D.; Haq, Z. Low density porous cross-linked polymeric materials and their preparation. European patent 0060138 B1, September 3, 1986.
18. Sing, K. S. W.; Everett, D. H., Haul, R. A. W.; Moscou, L.; Pierotti, R. A.; Rouquérol, J.; Siemieniewska, T. Reporting physisorption data for gas/solid systems with Special Reference to the Determination of Surface Area and Porosity. *Pure & Appl. Chem.* **1985**, *57*, 603-619.

19. Esquena, J.; Solans, C. *Highly Concentrated Emulsions as Templates for Solid Foams (Chapter 6), in: Emulsions Stability*, 2nd ed.; Boca Raton, FL, Taylor & Francis (Surfactant Science Series, Volume 132): USA, 2006.
20. López-Goerne, T. M. Nanotecnología y nanomedicina: la ciencia del futuro… hoy, 1st ed.; Arkhé: México, 2011.
21. Dean-Mo, L.; Troczynski, T.; Wenjea J. T. Water-based sol-gel synthesis of hydroxyapatite: process development. *Biomater.* **2001**, *22*, 1721-1730.
22. Vila, M.; Izquierdo-Barba, I.; Bourgeois, A.; Vallet-Regí, M. Bimodal meso/macro porous hydroxyapatite coatings. *J. Sol-Gel Sci. Technol.* **2011**, *57*, 109-113.
23. Sánchez-Salcedo, S.; Vila, M.; Izquierdo-Barba, I.; Cicuéndez, M.; Vallet-Regí, M. Biopolymer-coated hydroxyapatite foams: a new antidote for heavy metals intoxication. *J. Mater. Chem.* **2010**, *20*, 6956-6961.
24. Brezesinski T.; Groenewolt, M.; Gibaud, A.; Pinna, N.; Antonietti, M.; Smarsly, B. M. Evaporation-Induced Self-Assembly (EISA) at Its Limit: Ultrathin, Crystalline by Templating of Micellar Monolayers. **2006**, *18*, 2260-2263.
25. Vila, M.; Sánchez-Salcedo, S.; Cicuéndez, M.; Izquierdo-Barba, I.; Vallet-Regí, M. Novel biopolymer-coated hydroxyapatite foams for removing heavy-metals from polluted water. *J. Hazard. Mater.* **2011**, *192*, 71-77.
26. Jones, R. G.; Wilks, E. S.; Val Metanomski, W.; Kahovec, J.; Hess, M.; Stepto, R.; Kitayama, T. *Compendium of Polymer Terminology and Nomenclature (IUPAC Recommendations 2008)*, 2nd ed.; RSC Publishing: Cambridge, 2009.
27. Yang, X.; Guo, L.; Fan, Y.; Zhang, X. Preparation and characterization of macromolecule cross-linked collagen hydrogels for chondrocyte delivery. *Int. J. Biol. Macromol.* **2013**, *61*, 487-493.
28. Shyamkuwar, A. L.; Chokashi, K. P.; Waje, S. S.; Thorat, B. N. Synthesis, Characterization, and drying of absorbible Gelatin. *Drying Technol.* **2010**, *28*, 659-668.
29. Bigi, A.; Cojazzi, G.; Panzzvolta, S.; Roveri, N.; Rubini, K. Stabilization of gelatin films by crosslinking with genipin. *Biomater.* **2002**, *23*, 4827-4832.
30. Vílchez, S.; Samitier, V.; Porras, M.; Esquena, J.; Erra, P. Chitosan Hydrogels Covalently crosslinked with a Natural Reagent. *Tenside Surf. Det.* **2009**, *46*, 1-5.
31. Nishi, C.; Nakajima, N.; Ikada, Y. In vitro evaluation of cytotoxicity of diepoxy compounds used for biomaterial modification. *J. Biomed. Mater. Res.* **1995**, *29*, 829-834.
32. Mi, F.; Sung, H.; Shyu, S. Synthesis and characterization of a novel chitosan-based network prepared using naturally occurring crosslinker. *J. Polym. Sci., Part A: Polym. Chem.* **2000**, *38*, 2804-2814.
33. Butler, M. F.; Ng, Y.; Pudney, P. D. A.; Mechanism and kinetics of the crosslinking reaction between biopolymers containing primary amine groups and genipin. *J. Polym. Sci., Part A: Polym. Chem.* **2003**, *41*, 3941-3953.
34. Sundararaghavan, H. G.; Monteiro, G. A.; Lapin, N. A.; Chabal, Y. J.; Miksan, J. R.; Shreiber, D. I. Genipin-induced changes in collagen gels: correlation of mechanical properties to fluorescence. *J. Biomed. Mater. Res. A* **2008**, *87*, 2, 308-320.
35. Liang, H.; Chang, H.; Liang, H.; Lee, M.; Sung, H. Crosslinking Structures of Gelatin Hydrogels Crosslinked with Genipin or a Water-Soluble Carbodiimide. *J. Appl. Polym. Sci.* **2004**, *91*, 4017-4026.
36. Hall, S. J. *Basic Biomechanics*, 5th ed.; McGraw-Hill Higher Education: New York, 2007.
37. Cicuéndez, M.; Izquierdo-Barba, I.; Sánchez-Salcedo, S.; Vila, M.; Vallet-Regí, M. Biological performance of hydroxyapatite-biopolymer foams: In vitro cell response. *Acta Biomater.* **2012**, *8*, 802-810.
38. Colilla, M.; Manzano, M.; Vallet-Regí, M. Recent advances in ceramic implants as drug delivery Systems for biomedical Applications. *Int. J. Nanomedicine* **2008**, *3*, 4, 403-414.
39. Salinas, A. J.; Vallet-Regí, M. Bioactive ceramics: from bone grafts to tissue engineering. *RSC Adv.* **2013**, *3*, 11116-11131.

40. García-Garduño, M. V.; Reyes-Gasga, J. La hidroxiapatita, su importancia en los tejidos mineralizados y su aplicación biomédica. *TIP Rev. Esp. Cienc. Quím. Biol.* **2006**, *9*, 2, 90-95.
41. Turner, C. H.; Wang, T.; Burr, D. B. Shear strength and fatigue properties of human cortical bone determined from pure shear tests. *Calcif. Tissue Int.* **2001**, *69*, 373-378.
42. Yao, C.; Liu, B.; Chen, Y. Calvarial bone response to a tricalcium phosphate-genipin crosslinked gelatin composite. *Biomater.* **2005**, *26*, 3065-3074.
43. Hijón, N.; Cabañas, M. V.; Izquierdo-Barba, I.; Vallet-Regí, M. Bioactive Carbonate-Hydroxyapatite Coatings Deposited onto Ti_6Al_4V Substrate. *Chem. Mater.* **2004**, *16*, 1451-1455.
44. Rodríguez-Lorenzo, L. M.; Vallet-Regí, M.; Ferreira, J. M. F. Colloidal processing of hydroxyapatite. *Biomater.* **2001**, *22*, 1847-1852.
45. Padilla, S.; Román, J.; Vallet-Regí, M. Synthesis of porous hydroxyapatites by combination of gelcasting and foams burn out methods. *J. Mater. Sci. - Mater. Med.* **2002**, *13*, 1193-1197.
46. Ramsay, J. D. F. Colloidal properties of synthetic hectorite clay dispersions. I. Rheology. *J. Colloid Interface Sci.* **1986**, *109*, 441-447.
47. Sohm, R.; Tadros, T. F. Viscoelastic properties of sodium montmorillonite (Gelwhite H) suspensions. *J. Colloid Interface Sci.* **1989**, *132*, 62-71.
48. Tadros, T. F. Use of viscoelastic measurements in studying interactions in concentrated dispersions. *Langmuir* **1990**, *6*, 28-35.
49. Tadros, T. F.; *Rheology of dispersions: Principles ans Applications*, 1st ed.; Wiley-VCH: Weinheim, 2010.
50. Barnes, H. A.; Hutton, J. F.; Walters, K. *An introduction to Rheology (Rheology Series 3)*, 1st ed.; Elsevier Science: Amsterdam, 1989.
51. Brummer, R. *Rheology essentials of cosmetic and food emulsions*, 1st ed.; Springer-Verlag: Berlin, Heidelberg, 2006.
52. Rehman I.; Bonfield, W. Characterization of hydroxyapatite and carbonated apatite by photo acoustic FTIR spectroscopy. *J. Mater. Sci. - Mater. Med.* **1997**, *8*, 1-4.
53. Berzina-Cimdina, L.; Borodajenko, N. *Research of Calcium Phosphates Using Fourier Transform Infrared Spectroscopy, Infrared Spectroscopy – Materials Science, Engeneering and Technology*, 1st ed.; Prof. Theophanides Theophile (Ed.), InTech: Rijeka, 2012.
54. Agrawal, K.; Singh, G.; Puri, D.; Prakash, S. Synthesis and Characterization of Hydroxyapatite Powder by Sol-Gel Method for Biomedical Application. *J. Mater. Miner. Charact. Eng.* **2011**, *10*, 727-734.

8. ACRONYMS

EISA – Evaporation-induced self-assembly

EtOH – Ethanol

F127 – Pluronic® F 127 NF

FTIR or FT-IR – Fourier transform infrared spectroscopy

GP – Genipin

HAp – Hydroxyapatite

HLB – Hydrophilic-lipophilic balance

LVR – Linear viscoelastic region or linear viscoelasticity region

O/W (emulsion) – Oil-in-water (emulsion)

PBS – Phosphate buffered saline

rpm – Revolutions per minute

r. t. – Room temperature

S/A (emulsion) – Surfactant-in-alcohol (emulsion)

SEM – Scanning electron microscopy

TIP – Triethyl phosphite

W/O (emulsion) – Water-in-oil (emulsion)

XRD – X-ray diffraction